Journal of ELECTRONIC MATERIALS, Vol. 39, No. 11, 2010
DOI: 10.1007/s11664-010-1347-5

Effects on Undercooling and Interfacial Reactions with Cu Substrates of Adding Bi and In to Sn-3Ag Solder

YU-YAN CHIANG,[1] ROBBIN CHENG,[2] and ALBERT T. WU[2,3]

1.—Institute of Materials Science and Engineering, National Central University, Jhongli City 320, Taiwan. 2.—Department of Chemical and Materials Engineering, National Central University, Jhongli City 320, Taiwan. 3.—e-mail: atwu@ncu.edu.tw

This study investigated the effects of adding Bi and In to Sn-3Ag Pb-free solder on undercooling, interfacial reactions with Cu substrates, and the growth kinetics of intermetallic compounds (IMCs). The amount of Sn dominates the undercooling, regardless of the amount or species of further additives. The interfacial IMC that formed in Sn-Ag-Bi-In and Sn-In-Bi solders is Cu_6Sn_5, while that in Sn-Ag-In solders is $Cu_6(Sn,In)_5$, since Bi enhances the solubility of In in Sn matrices. The activation energy for the growth of IMCs in Sn-Ag-Bi-In is nearly double that in Sn-Ag-In solders, because Bi in the solder promotes Cu dissolution. The bright particles that form inside the Sn-Ag-In bulk solders are the ζ-phase.

Key words: Sn-Ag, Pb-free solder, bismuth, indium, growth kinetics

INTRODUCTION

Pb-containing solder is being phased out for environmental reasons. An ideal Pb-free solder should have similar properties to those of eutectic Sn-Pb solder, such as melting temperature, mechanical properties, and wettability. Most Pb-free solder alloys have much higher melting temperatures than that of eutectic Sn-Pb solder. In recent years, Sn-Ag-Cu solder systems have been extensively adopted in industry because they are reliable. However, their processing temperatures exceed 217°C, more than 30°C higher than that of eutectic Sn-Pb solder. This high melting temperature has a strong effect on the assembly of electronic packaging.

Adding In to Pb-free solder is known to reduce its melting temperature greatly. Kim and Tu[1] stated that Au dissolves more slowly in Sn-2.8Ag-20In solder than in other Sn-based solders. Sharif and Chan[2] found that Cu dissolves slowly in SAC305 solder to which 9 wt.% In is added. Chuang et al.[3] examined the interfacial reaction of Sn-2.8Ag-20In with Ni substrates. They found two phases of $Ni_3(Sn,In)_4$ formed at the interfaces in two different temperature ranges. In the lower temperature range (225°C to 275°C), the rate-limiting process is lattice diffusion of Ni through the dense intermetallic compound (IMC) layer; in the higher temperature range (300°C to 350°C), ripening governed the growth kinetics. Huang and Wang[4] reported that the addition of a little In (<5 wt.%) increases tensile strength but reduces ductility. Yeh[5] suggested that adding over 15 wt.% In leads to the formation of In-rich phases; it also affects the ultimate tensile strength and elongation. The addition of Bi also reduces the melting temperature. Various groups have studied the properties of Sn-Ag-Bi solders on Cu substrates. He and Acoff[6] showed that precipitation of Bi particles on grains and pinning at grain boundaries reduces the growth rate of interfacial IMCs between Sn-3.7Ag-*x*Bi solders and Cu substrates. The effect of adding Bi on the thermal and mechanical properties of Sn-Ag-Bi solders has been explored extensively.[7–12] If In and Bi are both added to Sn-Ag solders, they compensate for each other, helping to maintain good mechanical properties.[13,14] Based on the literature, this investigation compares the interfacial reactions, the IMC growth kinetics, and the thermal properties of these Sn-Ag-In and Sn-Ag-Bi solders, which react with Cu substrates, with reference to both kinetics and thermodynamics.

(Received March 30, 2010; accepted July 31, 2010; published online September 2, 2010)

The relevant data are compared with our previously reported data concerning Sn-Ag-Bi-In solders.[15,16]

This paper first discusses the effect of composition on the thermal properties of Sn-Ag-In, Sn-Ag-Bi, and Sn-Ag-Bi-In solders. Second, the interfacial reactions of Sn-Ag-Bi and Sn-Ag-In solders on Cu substrates and the growth kinetics of the interfacial IMCs are investigated. The kinetics of the growth of IMCs at various reflow temperatures and periods of reflow in a reflow experiment are calculated. The Arrhenius equation was used to calculate the activation energy of the growth of IMCs. The IMCs that were present in the solder were either Cu_6Sn_5 or the ζ-phase. In the final part of this study, the composition of the particles within the bulk solders is discussed.

EXPERIMENTAL PROCEDURES

Different weight percentages of In and Bi were melted with Sn-Ag solders to generate 94Sn-3Ag-3Bi, 84Sn-3Ag-3Bi-10In, 94Sn-3Ag-3In, and 80Sn-3Ag-17In alloys. Thirty milligrams of each of the solders was weighed out and placed in an Al crucible. The thermal properties of the samples were measured using a differential scanning calorimeter (DSC, Perkin-Elmer Diamond). The heating and cooling cycle rates were 10°C/min. The melting points were determined from the onset temperatures of all the solders. Two samples of each composition were tested for one thermal cycle. The onset temperatures in the first heating cycle were within 1°C of each other. Upon cooling, the onset temperatures of samples with the same composition were within 5°C of each other.

Thirty milligrams of 94Sn-3Ag-3In and 80Sn-3Ag-17In solders were reflowed on Cu coupons with dimensions of 10 mm × 10 mm in rosin mildly activated-type flux at 212°C, 222°C, 232°C, 242°C, and 252°C for 1 min, 5 min, 10 min, 20 min, and 40 min. Cu surfaces were pretreated by polishing using 0.1-μm and 1-μm Al_2O_3 suspensions. Samples were embedded in epoxy and cross-sectioned; scanning electron microscopy (FE-SEM, HITACHI S-4700) was applied to observe the cross-section of each sample to calculate the thicknesses of the interfacial IMCs. The average thickness of the interfacial IMC was calculated by measuring the area of the compounds and dividing by the total length of the image, averaging values from images at five locations to improve accuracy. Field-emission electron probe microanalysis (FE-EPMA, JEOL JXA-8500F) was carried out to determine the compositions of the compounds either at the interfaces or in the bulk solder.

RESULTS AND DISCUSSION

Thermal Analysis

Figure 1 shows the undercooling values of 94Sn-3Ag-3Bi, 94Sn-3Ag-3In, 80Sn-3Ag-17In, and 84Sn-3Ag-3Bi-10In solders. Table I summarizes the DSC results for these Pb-free solders. Heating and cooling were performed at 10°C/min. In the onset-to-onset method, undercooling is calculated as the onset temperature during heating minus the onset temperature associated with cooling.

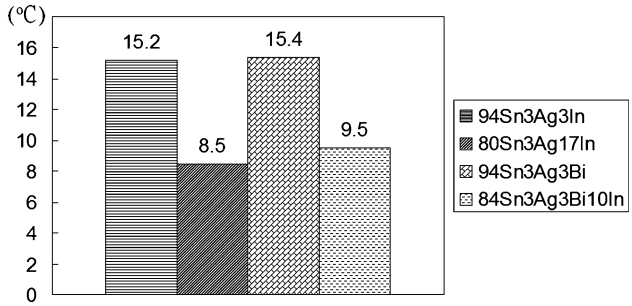

Fig. 1. Undercooling values of 94Sn-3Ag-3In, 80Sn-3Ag-17In, 94Sn-3Ag-3Bi, and 84Sn-3Ag-3Bi-10In solders. The heating and cooling cycle rates were 10°C/min.

Table I. DSC results of various Pb-free solders investigated

Composition (wt.%)	Onset *T* (Heating) (*T*1) (°C)	Onset *T* (Cooling) (*T*2) (°C)	Δ*T* (*T*1 − *T*2)
94Sn-3Ag-3In	212.61	197.40	15.21
80Sn-3Ag-17In	186.21	177.71	8.50
94Sn-3Ag-3Bi	214.70	199.35	15.35
84Sn-3Ag-3Bi-10In	193.70	184.23	9.47

As presented in Fig. 1, the degree of undercooling appears to be proportional to the amount of Sn in the solder. Some researchers have suggested that the addition of small amounts of alloying elements tends to be associated with small undercooling, since such elements may serve as extra heterogeneous nucleation sites and promote solidification.[17,18] Both 94Sn-3Ag-3Bi and 94Sn-3Ag-3In solders have similar undercooling values; the undercooling values obtained by adding Bi and In are very similar for a given Sn content. The results indicate that Sn is the element that dominates undercooling behavior. Furthermore, the undercooling of 94Sn-3Ag-3In exceeds that of 80Sn-3Ag-17In, verifying that the undercooling increases with the Sn content. Moreover, added In atoms not only substitute at the Sn sites to form IMCs at the interfaces or in the solder, but also precipitate together with Ag and Sn to form small particles that were identified as the ζ-phase. These particles may be the primary phase that forms upon cooling. Another possible primary phase in the solder may be Cu_6Sn_5 particles. Although the DSC cooling curve includes a single major peak, the onset temperature of cooling increased with the amount of Sn. The difference between the onset temperatures of

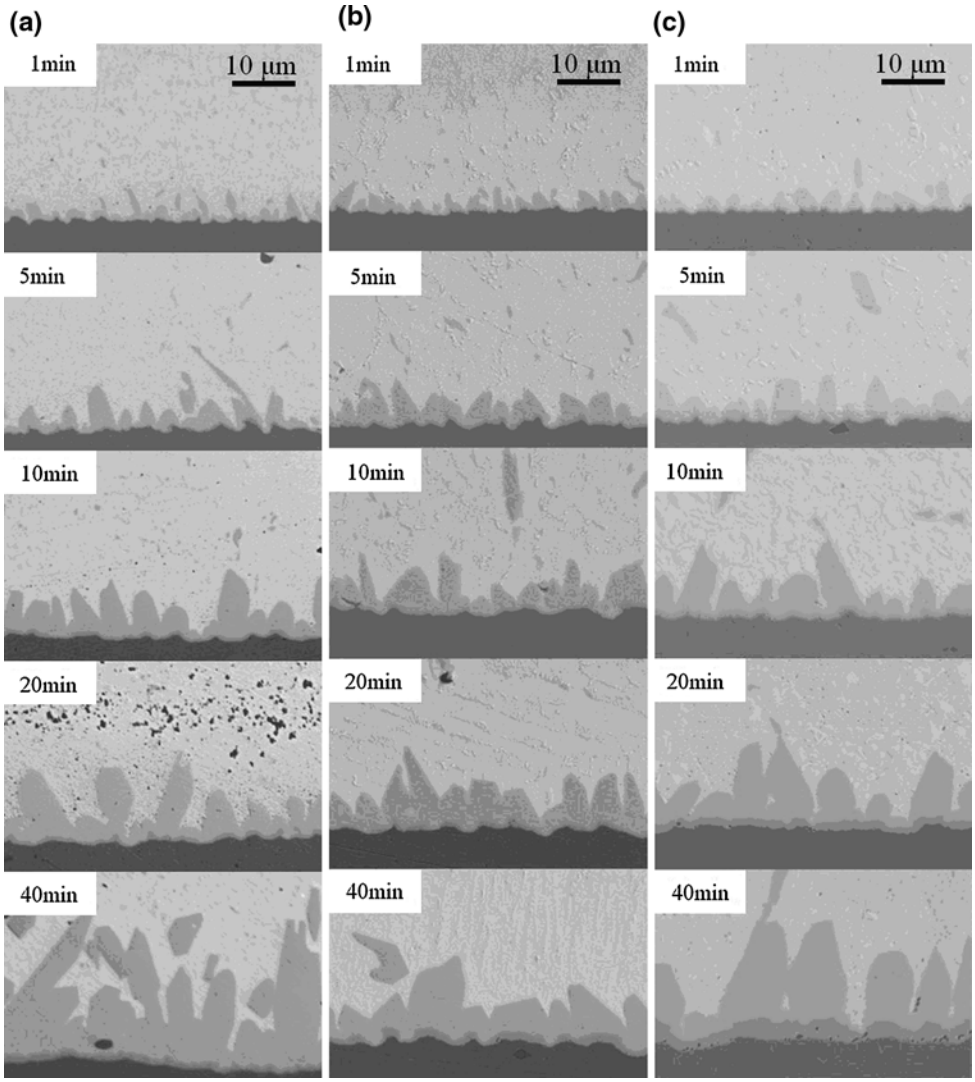

Fig. 2. Cross-sectional SEM images of the interface between (a) 94Sn-3Ag-3Bi, (b) 94Sn-3Ag-3In, and (c) 80Sn-3Ag-17In solders and Cu substrates after reflow at 252°C for various times.

94Sn-3Ag-3Bi and 94Sn-3Ag-3In was only about 1°C. However, the difference was 4°C for 84Sn-3Ag-3Bi-10In and 5°C for 80Sn-3Ag-17In. The differences in the onset temperatures are caused by the solidification of the primary phases. Additionally, the primary phases may not have provided suitable sites for heteronucleation of Sn, so the undercooling value of the solder increases with Sn content.

Kinetics of Formation of Interfacial IMCs

Figure 2 presents selected images of IMCs between 94Sn-3Ag-3In, 80Sn-3Ag-17In, and 94Sn-3Ag-3Bi solders on Cu substrates at 252°C for different durations of time. These images show that the IMCs are composed of two layers. Elemental analysis by EPMA revealed that the layers between Cu substrates and 94Sn-3Ag-3Bi solders were very similar to those found for most Sn-based Pb-free solders. These layers are ε- and η-phases, which are Cu_3Sn and Cu_6Sn_5, respectively. However, analysis of the Sn-Ag-In solders revealed that the layers above the Cu substrates were ε and η, with In atoms substituted at the lattice sites of Sn, because they have similar physical properties. The ε-phases in all of the solders grew linearly with $t^{1/2}$ in a diffusion-controlled process. The η-phases grew and the amount of scallop-shaped compounds decreased as the reflow time or temperature increased. In the images in Fig. 2, the η-phases are prominent, especially in samples that were reflowed at high temperature for long time. Moreover, the η-phases are brittle and reduce the mechanical strength of the solder joints. Hence, the Cu_6Sn_5 and $Cu_6(Sn,In)_5$ layers were considered in order to elucidate the growth kinetics. Figure 3 plots the thickness of η-phases in the Sn-Ag-In, Sn-Ag-Bi, and Sn-Ag-Bi-In solders versus reflow time at various temperatures.

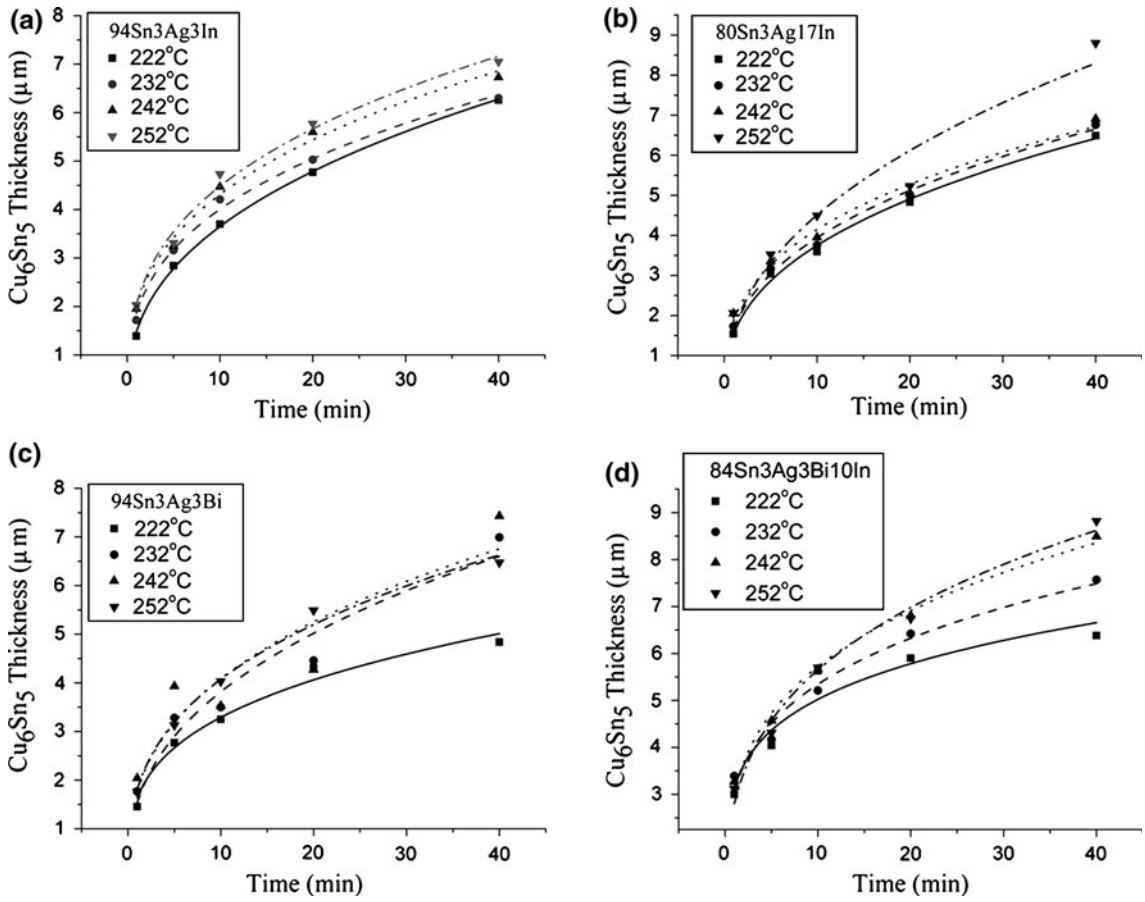

Fig. 3. The thickness of η-phase versus reflow time at different reflow temperatures in (a) 94Sn-3Ag-3In, (b) 80Sn-3Ag-17In, (c) 94Sn-3Ag-3Bi, and (d) 84Sn-3Ag-3Bi-10In solders.

Table II. Time exponent values, *n*, of Sn-Ag-In and Sn-Ag-Bi solders after reflow at various temperatures

Solder	222°C	232°C	242°C	252°C
94Sn-3Ag-3In	0.36	0.33	0.33	0.35
80Sn-3Ag-17In	0.34	0.33	0.37	0.34
94Sn-3Ag-3Bi	0.43	0.27	0.31	0.37

The relationship between the compound thickness and the reflow time is given by

$$w = kt^n,$$

where w represents the thickness of the η IMCs, t is the reflow time, and k is a growth constant. Plotting the thickness of the layers as a function of reflow time yields the time exponent n. Table II presents the mean n values of both solders. The time exponents n in both solders are close to 1/3. The results demonstrate that the growth of both Cu_6Sn_5 and $Cu_6(Sn,In)_5$ is ripening controlled, as in most Sn-free solder systems. The phases of scallop-shaped compounds grew, but the amount declined as the duration of reflow increased.

Cu diffusion from the substrates to the solders and surface diffusion for ripening are critical to compound growth. This growth is known to be a thermally activated process. The growth constant k can be written as

$$k = k_0 x \exp(-Q/RT).$$

The slope of the natural logarithm of k against $1/T$ yields the activation energy of $Cu_6(Sn,In)_5$. Figure 4 plots the activation energies of all the solders. All lines are the best fit by linear regression with a confidence level of 95%. According to Fig. 4, the activation energies of the scallop IMC growth in both Sn-Ag-In solders are very similar, while that in Sn-Ag-Bi solder is slightly higher. The data points in Fig. 4 for the compound thickness of 84Sn-3Ag-3Bi-10In at $1000/T(\mathrm{K}) = 2.02$ and 94Sn-3Ag-3Bi at $1000/T(\mathrm{K}) = 1.98$ are not on the lines. However, these data points were determined from the average thickness. To the best of our knowledge, these data points are still valid. The results shown in Fig. 4 are consistent with the argument that the addition of Bi inhibits the growth of IMCs. The authors have already extensively investigated the interfacial reactions between Sn-Ag-Bi-In solders and Cu

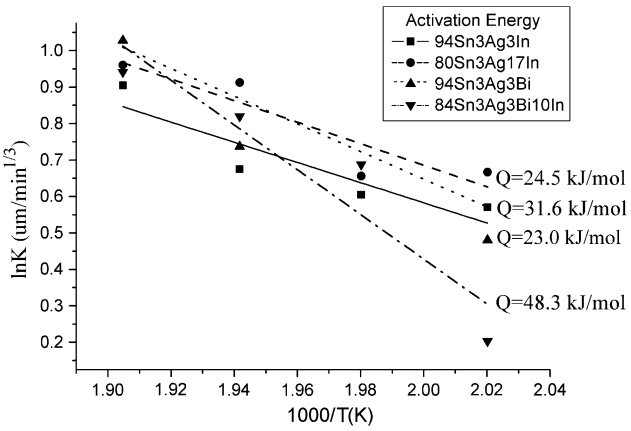

Fig. 4. Activation energies of interfacial IMCs in Sn-Ag-In, Sn-Ag-Bi, and Sn-Ag-Bi-In solders.

Table III. EPMA results of the interfacial IMCs between Sn-Ag-In and Sn-Ag-In-Bi solders with Cu substrates after reflow at 252°C for 40 min

EPMA (at.%)	Cu	Sn	Ag	In
94Sn-3Ag-3In	53.3	45.3	0.3	1.2
80Sn-3Ag-17In	55.4	38.4	0.3	5.9
84Sn-3Ag-3Bi-10In	56.9	43.1	–	–

substrates.[15,16] Intriguingly, the activation energies of IMC growth in Sn-Ag-In solders are only half of that in Sn-Ag-Bi-In. The addition of Bi seemingly increased the barrier to compound formation and may have enhanced the solubility of Cu in Sn-Ag-Bi-In solder. Consequently, saturation of Cu becomes more difficult. The nucleation and growth of Cu-Sn compounds depend on the oversaturation of Cu. Until the saturation concentration is reached, IMCs cannot precipitate. Additionally, Table III presents EPMA results for the atomic compositions of the IMC at the solder/Cu interfaces in all the solders, revealing that Cu_6Sn_5 formed in Sn-Ag-Bi-In solders whereas $Cu_6(Sn,In)_5$ formed in Sn-Ag-In solders. The ternary phase diagram of Sn-Bi-In indicates that the addition of a small amount of Bi increases the solubility of In in Sn.[19,20] Our results suggest that In stayed in the Sn-Ag-Bi-In solder matrices during reflow and did not participate in the formation of interfacial IMCs. In contrast, the In content oversaturated near the solder/Cu interfaces with no Bi. In then precipitated together with Sn atoms to form $Cu_6(Sn,In)_5$, in which In atoms substituted at Sn atomic sites.

ζ-Phase

In Fig. 2b and c, numerous bright particles were dispersed in Sn-Ag-In but not in Sn-Ag-Bi solder matrices. These bright particles were investigated by EPMA. Only data concerning the solders reflowed on Cu substrates at 252°C for 40 min are presented. Table IV presents the compositions of the particles.

Table IV. EPMA results of bright particles in Sn-Ag-In and Sn-Ag-Bi-In solders after reflow at 252°C for 40 min

EPMA (at.%)	Sn	Ag	In
94Sn-3Ag-3In	19.4	67.1	12.8
80Sn-3Ag-17In	2.0	66.5	30.2
84Sn-3Ag-3Bi-10In	10.8	67.8	20.4

The EPMA results demonstrate that these bright particles comprised In, Ag, Sn, and a small amount of Cu. In the Sn-Ag-In phase diagram,[21–23] no such ternary compound exists. The compositions of these particles are located in the ζ-phase region, in which Ag_4Sn and Ag_3In form a solid solution, since they have the same crystal structure. According to Liu et al.,[22] the ζ-phase is a hexagonal phase that exists over a broad range of compositions from the Ag-Sn side to the In-Sn side of the ternary diagram. These bright particles have also been found in Sn-Ag-Bi-In solder, and are also identified as the ζ-phase.[15,16] These results suggest that ζ-phase particles are the most stable IMCs that form in Sn-Ag-In solder reactions with Cu substrates, regardless of whether Bi is present.

CONCLUSIONS

This study investigated the thermal and interfacial reactions of Sn-Ag-based solder to which In and Bi were added. Undercooling of the solders was affected by the added elements but was dominated by the amount of Sn. The IMC that formed at the interfaces between Sn-Ag-In solder and Cu substrates was $Cu_6(Sn,In)_5$, whereas that formed between Sn-Ag-Bi-In and Cu was Cu_6Sn_5. Addition of Bi enhanced the dissolution of In in Sn. The activation energy of interfacial IMCs in Sn-Ag-Bi-In was double that in Sn-Ag-In solder, since the addition of Bi increases the rate of dissolution of Cu in the solder. The bright particles in the bulk solder were the ζ-phase.

ACKNOWLEDGEMENTS

The authors would like to acknowledge financial support from the National Science Council of Taiwan. The help of S.Y. Tsai from National Tsing Hua University with operating the EPMA is greatly appreciated.

REFERENCES

1. P.G. Kim and K.N. Tu, *Mater. Chem. Phys.* 53, 165 (1998).
2. A. Sharif and Y.C. Chan, *J. Alloys Compd.* 390, 67 (2005).
3. T.H. Chuang, K.W. Huang, and W.H. Lin, *J. Electron. Mater.* 33, 374 (2004).
4. M.L. Huang and L. Wang, *Metall. Mater. Trans. A* 36A, 1439 (2005).

5. M.S. Yeh, *Metall. Mater. Trans. A* 34A, 361 (2003).
6. M. He and V.L. Acoff, *J. Electron. Mater.* 37, 288 (2008).
7. Y. Kariya and M. Otsuka, *J. Electron. Mater.* 27, 1229 (1998).
8. P.T. Vianco and J.A. Rejent, *J. Electron. Mater.* 28, 1138 (1999).
9. P.T. Vianco and J.A. Rejent, *J. Electron. Mater.* 28, 1127 (1999).
10. C.W. Hwang, J.G. Lee, K. Suganuma, and H. Mori, *J. Electron. Mater.* 32, 52 (2003).
11. S.W. Shin and J. Yu, *J. Electron. Mater.* 34, 188 (2005).
12. M. Kamal, E.S. Gouda, and L.K. Marei, *Cryst. Res. Technol.* 44, 1308 (2009).
13. K.S. Kim, T. Imanishi, K. Suganuma, M. Ueshima, and R. Kato, *Microelectron. Reliab.* 47, 1113 (2007).
14. R.K. Shiue, L.W. Tsay, C.L. Lin, and J.L. Ou, *J. Mater. Sci.* 38, 1269 (2003).
15. A.T. Wu, M.H. Chen, and C.H. Huang, *J. Alloys Compd.* 476, 436 (2009).
16. A.T. Wu, M.H. Chen, and C.N. Siao, *J. Electron. Mater.* 38, 252 (2008).
17. K.-W. Moon, W.J. Boettinger, U.R. Kattner, F.S. Biancaniello, and C.A. Handwerker, *J. Electron. Mater.* 29, 1122 (2000).
18. S.K. Kang, M.G. Cho, P. Lauro, and D.Y. Shih, *Proceedings of the 57th ECTC* (2007), p. 1597.
19. V.T. Witusiewicz, U. Hecht, B. BÖttger, and S. Rex, *J. Alloys Compd.* 428, 115 (2007).
20. I. Ohnuma, Y. Cui, X.J. Liu, Y. Inohana, S. Ishihara, H. Ohtani, R. Kainuma, and K. Ishida, *J. Electron. Mater.* 29, 1113 (2000).
21. S.W. Chen, C.H. Wang, S.K. Lin, and C.N. Chiu, *J. Mater. Sci. Mater. Electron.* 18, 19 (2006).
22. X.J. Liu, Y. Inohana, Y. Takaku, I. Ohnuma, R. Kainuma, K. Ishida, Z. Moser, W. Gasior, and J. Pstrus, *J. Electron. Mater.* 31, 1139 (2002).
23. T.M. Korhonen and J.K. Kivilahti, *J. Electron. Mater.* 27, 149 (1998).